This is the accepted version of:
A. Nespoli, P. Bettini, E. Villa, G. Sala, F. Passaretti, A.M. Grande
A Study on Damping Property of Niti Elements Produced by Selective Laser-Beam Melting
Advanced Engineering Materials
doi:10.1002/adem.202001246
The final publication is available at https://doi.org/10.1002/adem.202001246

A study on damping property of NiTi elements produced by selective laser beam melting

Adelaide Nespoli, Paolo Bettini, Elena Villa, Giuseppe Sala, Francesca Passaretti, Antonio Mattia Grande*

Dr. Adelaide Nespoli, Dr. Elena Villa, Dr. Francesca Passaretti

Consiglio Nazionale delle Ricerche – Istituto di Chimica della Materia Condensata e di Tecnologie per l'Energia (CNR-ICMATE), via G. Previati 1/e 23900 Lecco (Italy)

E-mail: adelaide.nespoli@cnr.it

Prof. Paolo Bettini, Prof. Giuseppe Sala, Prof. Antonio Mattia Grande

Politecnico di Milano – Dipartimento di Scienze e Tecnologie Aerospaziali, via La Masa 34 20156 Milano (Italy)

Keywords: damping; loss factor; NiTi; selective laser beam melting, additive manufacturing

The damping properties of NiTi elements produced through selective laser melting are investigated by tuning the process parameters. To this end, twelve parameters' sets are selected to fabricate fully-dense NiTi specimens. Damping is evaluated through loss factor index, mechanical loading cycles (up to 10^4 cycles), solicitation frequency and strain amplitude. Results confirm that NiTi fabricated through selective laser beam melting is an excellent candidate to substitute conventional materials when used in the martensite phase. Furthermore, the selected process parameters enable specific damping performances that can be collected in damping maps which turn out to be practical tools for the fabrication of NiTi parts with tunable damping response.

This is the accepted version of:
A. Nespoli, P. Bettini, E. Villa, G. Sala, F. Passaretti, A.M. Grande
A Study on Damping Property of Niti Elements Produced by Selective Laser-Beam Melting
Advanced Engineering Materials
doi:10.1002/adem.202001246
The final publication is available at https://doi.org/10.1002/adem.202001246

1. Introduction

NiTi is the most common and industrially exploited multifunctional alloy thanks to its unique features: shape memory effect and pseudoelasticity. These two properties enable a mechanical work that is frequently used in many applications to generate motion, both for actuation and sensing, or to dissipate energy, like in dampers. At the base of these mechanical attitudes exhibited by NiTi there is a first-order thermoelastic transformation between two solid phases, martensite and austenite, which are respectively stable at low and high temperature ranges. The transformation between martensite and austenite can be either thermally or stress induced[1] and it can be successfully used in several engineering applications. Among others, NiTi components are employed to preserve instrumentations and sensitive equipment from environmental noise and structural vibrations. [2 – 8] The practical applications of NiTi dampers are usually under isothermal conditions and may involve either low or high strain amplitudes, encouraging two different methodologies of investigation, accordingly.

1.1 NiTi damping at low strain amplitudes

Under low cyclic strain, in the order of 0.1 - 0.001 %, damping is linked to the internal friction that can be evaluated by temperature depending transformations, IF(T). In this situation, the phase transformation is exploited as an energy dissipation process and it is characterized by the intrinsic, $IF_{int}(T)$, the transitory, $IF_{tr}(T)$, and the phase transition, $IF_{pt}(T)$, components[9,10]: $IF(T)= IF_{int}(T)+ IF_{tr}(T)+ IF_{pt}(T)$.

The intrinsic term only depends on the microstructure and it gives the contribution of martensite and austenite. Martensite phase shows a relatively high intrinsic internal friction[9], which is mainly ascribed to the stress-induced viscous motion of variant interfaces and twin boundaries. Internal variables, such as the type of material, grain size, martensite interface density, defect structure as well as external parameters, such as temperature, time frequency and amplitude, can change the martensite damping capacity.[11] It was found that the internal friction of martensite can reach maximum values in the order of $8x10^{-2}$ at 10^{-2} % strain.[9] In

the austenite phase, the intrinsic term of the internal friction is usually very low as there are no mobile defects or interfaces.

The transitory term only appears during temperature variation. It is related to the kinetic effects and it is associated with the motion of austenite-martensite interfaces during the thermally induced transformation. It is the highest internal friction contribution and it depends on external parameters. This term becomes zero in isothermal conditions and so ineffective in the majority of practical applications where the temperature is kept constant.[9, 10] Furthermore, this term becomes negligible at ultrasonic solicitation frequencies.[12]

Finally, the phase transition term refers to the austenite-martensite transition and it is responsible for the internal friction maximum in isothermal conditions. A representative example of an internal friction measurement under cooling is reported in **Figure 1a.**

1.2 NiTi Damping at high strain amplitudes

Despite its low intrinsic term at low strains, austenite may exhibit high damping properties at strain amplitudes in the range from 4 to 8 % thanks to the occurrence of a stress induced phase transition from austenite to martensite, which takes place at constant temperature, higher than the austenite finish one. This transition, known as pseudoelasticity, is completely reversible and hysterical. This peculiar behavior is due to a stress-induced phase change of the material from the orderly and rigid austenite state into the more deformable martensite.[1] The material freely recovers the original austenite state once the load is removed since the stress-induced martensite is thermodynamically unstable at high temperature. This reversible phase change induces a characteristic hysteretic mechanical cycle through which the NiTi is dissipating passively a large amount of energy (see **Figure 1b**).[13] Proper thermo-mechanical processing and NiTi composition can maximize the transformation hysteresis, inducing high loading and low unloading plateaux.[7] Pseudoelastic NiTi is now deeply studied for those applications that involve large parts or assemblies such as buildings[14, 15] and space

This is the accepted version of:
A. Nespoli, P. Bettini, E. Villa, G. Sala, F. Passaretti, A.M. Grande
A Study on Damping Property of Niti Elements Produced by Selective Laser-Beam Melting
Advanced Engineering Materials
doi:10.1002/adem.202001246
The final publication is available at https://doi.org/10.1002/adem.202001246

structures[16 - 20], thanks to both the large superelastic strains (up to 8%) and the self-centering capability.

1.3 The loss factor as a measure of the damping property

The loss factor η is the most suitable index to describe the damping properties of NiTi. It was firstly introduced as a measure of intrinsic damping of viscous materials[21]:

$$\eta = \frac{E''}{E'} \quad (1)$$

where E'' and E' are the loss and the storage modulus, respectively. Alternatively, a definition in terms of energy can be used[9, 21]:

$$\eta = \frac{W}{2 \cdot \pi \cdot W_{load}} \quad (2)$$

where W is the energy lost during a cycle of loading and unloading (generally converted into heat) and W_{load} is the mechanical energy stored during the loading path.

1.4 Additive manufacturing of NiTi

The advantage to produce near net components through additive manufacturing technologies allows to overcome several issues that make the conventional methods ineffective in the production of high-quality complex NiTi components.[22 -28] Among the known additive manufacturing processes, selective laser melting (SLM) uses a laser beam source to selectively melt micrometric metal powders, layer upon layer, to fabricate 3D objects.[29] Recently, SLM has become very attractive for the fabrication of NiTi components[30 - 34] and significant efforts have been mainly focused on the selection of the process parameters that maximize the thermo-mechanical performance.[35-42] With this regard, the control of energy input (E) is adopted as the main criteria to study the SLM process as it links different process parameters: $E = \frac{P}{t \cdot v \cdot h}$ (P is the laser power, t is the layer thickness, v is the scan speed and h is the hatch distance).[43] For NiTi alloys, values of E in the range of 55 to 222 J/mm^3 provide high density and low porosity level within the produced samples.[36-39, 44-48] Despite the extensive literature on NiTi components produced by SLM, many issues are still open or have

This is the accepted version of:
A. Nespoli, P. Bettini, E. Villa, G. Sala, F. Passaretti, A.M. Grande
A Study on Damping Property of Niti Elements Produced by Selective Laser-Beam Melting
Advanced Engineering Materials
doi:10.1002/adem.202001246
The final publication is available at https://doi.org/10.1002/adem.202001246

not been completely explored; so far, damping has received very little attention. An interesting work on damping is reported by Wang *et al.*[12] that found an excellent damping response of a layer-structured NiTi sample produced by alternating two sets of SLM process parameters during printing.

The present research is aiming to fill the gap of information about the damping properties of NiTi fabricated through SLM. For this purpose, a starting guideline to the selection of SLM process parameters that enable high damping levels at a given specific temperature is proposed.

2. Materials and Methods

Several NiTi bars (3x3x15 mm^3) were produced from a NiTi micrometric powder (TLS Spezialpuver gmbh) with 55.2 wt.% Ni (A_f = 28 °C[48]) through a Renishaw AM400 selective laser melting machine which works with a pulsed wave emission Ytterbium fiber laser. The process parameters were selected to obtain near fully dense and defect-free specimens accordingly to a previous study[48]: the laser power and the layer thickness were kept constant at 250 W and 30 µm respectively. Besides, three values of laser speed were considered (1000, 1250, 1500 mm/s) and four hatching distance values were investigated (50, 75, 100, and 120 µm). Prior to processing, the working chamber was filled with Argon and the oxygen level was kept lower than 500 ppm during the all manufacturing process. No preheating was applied to the building platform.

Damping at low strain amplitudes was evaluated through thermally-induced transformation measurements following Equation 1. The loss factor was evaluated through three-point bending measurements at 0.02 % strain by the Q800 (TA Instruments) in the [-70 °C; 130 °C] temperature range, at 2 °C/min heating/cooling rate and at frequencies of 0.5, 1 and 10 Hz. Samples were prepared in order to have a tape shape with length of 12 mm, width of 3 mm and thickness lower than 0.4 mm. The internal friction intrinsic terms, $IF_{int}(T)$, of martensite and austenite were evaluated through the loss factor measurement respectively at –70 °C and

This is the accepted version of:
A. Nespoli, P. Bettini, E. Villa, G. Sala, F. Passaretti, A.M. Grande
A Study on Damping Property of Niti Elements Produced by Selective Laser-Beam Melting
Advanced Engineering Materials
doi:10.1002/adem.202001246
The final publication is available at https://doi.org/10.1002/adem.202001246

130 °C, which are the temperatures where the two phases are certainly stable. Furthermore, the effect of the solicitation amplitude on the loss factor of martensite was investigated through three-point bending measurements at constant frequency (10 Hz) and with the strain varied in the range from 10^{-5} (10^{-3} %) to 10^{-3} (10^{-1} %). Before measurements**,** the samples were held isothermal at martensite finish temperature for 30 minutes to eliminate the transitory term.

Pseudoelasticity was studied through dynamic compression measurements at fixed temperature. In order to avoid buckling during compression tests, the height of each bar was reduced to 5 mm through a non-consumable diamond blade and the contacting surface were refined by means of metallographic grinding. Dynamic response was evaluated through an Instron Electropulse E3000 machine equipped with a thermal chamber; measurements were accomplished at A_f + 10 °C temperature (where A_f is the austenite finish temperature) at 4 % strain for 10^4 loading/unloading cycles and at a solicitation frequency of 1 and 3.5 Hz. For these high strain measurements, the loss factor was evaluated through the energetic approach (Equation 2). A_f was measured by differential scanning calorimetry (DSC, Q100 TA Instr.) with a heating/cooling rate of 10 °C/min in the [-120 °C; 150 °C] range over two cycles per sample. The tangent method was used to identify the characteristic transition temperatures.

3. Results

3.1 Thermally induced transformation

Figure 2 and **Figure 3** depict the maps of the loss factors of martensite and austenite at low strains, respectively, as a function of the SLM process parameters. Due to the viscous motion of martensite variant interfaces and twin boundaries, martensite presents an intrinsic internal friction component higher than the austenite one. Furthermore, Figure 2 highlights a large zone of process parameter pairs that enables high loss factor when the solicitation frequency is 0.5 Hz; the highest values are registered when the hatching distance is between 50 and 100 µm and the scanning speed is between 1000 and 1250 mm/s. At 1 Hz, only high *h* and *v*

values enable an acceptable loss factor. At 10 Hz the optimum loss factor zone is located at low hatching distance, 50 µm, and scanning speed of 1250 mm/s. As concerns the damping response of austenite at 0.5 Hz (see Figure 3), the highest loss factor values are identified in two distinct zones that are linked by the 100 µm -1000 mm/s and 120 µm - 1500 mm/s process parameters pairs. At 1 and 10 Hz, the optimum loss factor zones are highly reduced: at 1 Hz these zones are located at high scanning speed with hatching near to 70 and 120 µm. At 10 Hz, optimum loss factor regions are located both at low hatching and scanning speed values and at hatching of 120 µm and scanning speed of 1500 mm/s.

Figure 4 reports the intrinsic internal friction of martensite as function of the solicitation amplitude. Results are grouped under the *h* process parameter. It can be seen that the internal friction decreases with the increasing of *v* parameter at strains between 10^{-4} (10^{-2} %) and 10^{-3} (10^{-1} %). An almost unstable response was registered at strain near 10^{-5}.

3.2 Stress induced transformation

Austenite finish temperature (A_f) as a function of the process parameters is reported in **Table 1.** It worth to notice that the 12 parameters' sets enable an increasing of the transformation temperatures with respect to that of the feedstock powder (A_f = 28 °C) due to Ni loss during the process ascribed to both Ni evaporation and the formation of Ni-rich precipitates. [48]

Figure 5 reports a representative example of compression test taken at 1 Hz and at A_f + 10 °C. It can be noticed a narrow mechanical hysteresis.

Figure 6 and **Figure 7** depict the maps of the loss factor as a function of the process parameters (hatching distance and scanning speed) during the compression tests at 1 Hz and at 3.5 Hz, respectively. In these figures, cycle number 50, 10^3 and 10^4 are reported. A general decrease of performance is observable between 50 and 10^3 cycles at both solicitation frequencies, while negligible changes are noticeable between 10^3 and 10^4 cycles meaning that at 10^3 cycle the loss factor is stable. Moreover, the maps referred to the measurements taken at 1 Hz show the existence of a large range of process parameters that enable high damping

This is the accepted version of:
A. Nespoli, P. Bettini, E. Villa, G. Sala, F. Passaretti, A.M. Grande
A Study on Damping Property of Niti Elements Produced by Selective Laser-Beam Melting
Advanced Engineering Materials
doi:10.1002/adem.202001246
The final publication is available at https://doi.org/10.1002/adem.202001246

values. Besides, a more restricted area of high loss factor values is visible in the maps referred to 3.5 Hz measurements.

Combining the maps referred to 1 and 3.5 Hz measurements, it can be assumed that the pair composed by 100 µm of hatching and 1250 mm/s of scanning speed assures a high loss factor independently from both the solicitation frequency and the number of mechanical cycles. Furthermore, it can be seen that the loss factor values are comparable to those registered at low strain (Figure 1 and Figure 2) independently from the solicitation frequency, however they are associated to different process parameters pairs.

4. Discussions

The presented results show that NiTi parts fabricated through SLM may guarantee mechanical properties and dynamic characteristics suitable for damping vibrations spanning from low to high amplitude levels at low frequencies. The occurrence of Ni loss during the process [48] results in 12 NiTi families with specific microstructure, thermal characteristic (see A_f of **Table 1**) and damping response. **Figure 8** reports a comparison between the maximum loss factor of the studied NiTi parts and the one of different materials produced through traditional processing. Conventional materials (aluminum 99.7% purity, aluminum alloys, steel, standard brass, cast iron, copper 99.9% purity, grey cast iron, manganese alloys, OLC45 steel), hybrid materials (aluminum foams, aluminum corrugated sandwich, composite materials reinforced by carbon fibers CFRP) and shape memory alloys (CuZnAl, CuMnAl) were considered. Among the materials prepared from bulk, CuZnAl shape memory alloy presents the highest loss factor (0.035 [49]). Grey cast iron also presents a high loss factor (0.028 [49]) which is principally attributed to the presence of graphite that absorbs the energy and converts it into heat. Within hybrid materials, aluminum foams and corrugated sandwich components represent an innovative category of lightweight materials with relative high loss factor (0.01). Similar results were found for manganese alloys.[50] NiTi parts fabricated through SLM process present the highest loss factor (0.064) when working under high strain static operating

conditions thank to its pseudoelastic response. This value drastically decreases in dynamic conditions where loss factor values are 0.0088 at 1 Hz and 0.0085 at 3.5 Hz, slightly lower than those of aluminum foams and corrugated sandwich components. At low strains, NiTi as-built components present an excellent damping behavior when working at low temperature in martensite phase. The loss factor of martensite is similar within the three considered solicitation frequencies: 0.048 at 0.5 Hz, 0.050 at 1Hz, 0.045 at 10 Hz. It is worth noting that austenite shows a loss factor higher than 0.01 at the three considered frequencies performing better than both the hybrid aluminum materials (foams and corrugated sandwiches) and manganese alloys. High loss factor values were registered at the peak temperature of the phase transition upon both cooling and heating ramps: the maximum values were 0.0824 (at 35 °C) and 0.0634 (at 46 °C), respectively. It was found that both these peaks involved the rhombohedral phase since they are associated to the austenite-to-rhombohedral phase transition during cooling and to the rhombohedral-to-austenite transition during heating.

As opposed to standard materials, the loss factor of the NiTi components is strictly dependent from the working temperature. Indeed, low working temperatures should be considered to maximize the loss factor of martensite phase. On the other side, high temperatures should be taken into account when the austenite pseudoelastic behavior is involved.

The observed maximum loss factor values of NiTi parts were obtained by selecting precise SLM process parameters. **Table 2** summarizes the pairs of hatch distance, *h*, and scanning speed, *v*, values of NiTi parts fabricated through SLM. It can be noticed that there is a pair of process parameters shared by the great part of samples tested at low strain, h = 120 μm and v = 1500 mm/s, that maximize the loss factor. This suggests that these values are the most suitable parameters that maximized the damping properties at low strains of NiTi fabricated through SLM. Besides, at high strains and in dynamic working conditions, it was observed that the loss factor is maximized when h is 100 μm and v is 1000 mm/s or 1250 mm/s.

This is the accepted version of:
A. Nespoli, P. Bettini, E. Villa, G. Sala, F. Passaretti, A.M. Grande
A Study on Damping Property of Niti Elements Produced by Selective Laser-Beam Melting
Advanced Engineering Materials
doi:10.1002/adem.202001246
The final publication is available at https://doi.org/10.1002/adem.202001246

At high strain, the damping properties change upon mechanical cycling. Two main outcomes can be highlighted from these tests. First, the highest mechanical response was observed within the firsts 50 mechanical cycles and a stable functioning is mostly attained at 10^3 cycles. Secondly, despite a satisfactory loss factor and the stable and almost complete recovered strain, the dissipated energy observed at high strains (calculated as the area within a loading/unloading cycle) is low even at early mechanical cycles and it drastically decreases with mechanical cycling (see Supporting info for loss energy maps). Furthermore, the known stress plateau was substituted by a slope stress during both forward and reverse transformation. This aspect is more evident in dynamic functioning (see curves reported in **Figure 9**). Furthermore, there are two concurrent factors related to this trend. The as-built condition of the fabricated samples, which present a non-homogeneous ultrafine microstructure with precipitates, has a great impact on the amplitude of the pseudoelastic hysteresis since it obstacles the spring-back at the beginning of unloading. Besides, dynamic functioning causes an increase of the temperature field with a subsequently increase of the loads inducing the stress-induced phase transition. Comparing the results related to the dissipated energy at different frequencies, it can be furtherly noticed that there are not overlapping zones. All these considerations confirm that the mechanical behavior of NiTi alloys is characterized by a strong loading rate/ frequency dependence, due to heat generation, heat accumulation, heat transfer and the intrinsic temperature dependence of the transformation stress of the material (Clausius–Clapeyron relation).[51, 52] In dynamic functioning, precipitates also promote multi-domain martensite variants with different energetic barriers that reduce the difference of transition temperatures between loading and unloading cycles. For the Clausius-Clapeyron law, it results a more evident slope in the stress strain curve and a wider dispersion of stress values, even lower than the induced stress of the plateau. A narrowing of the mechanical hysteresis is consequently achieved. This effect is not visible in quasi static measurements where the effect of precipitates is less evident thanks to sufficient time to transfer the heat

generated during the phase transition and to give the possibility to induce martensitic domain at more stable energetic condition.

Finally, preliminary tests about the effects of low solicitation amplitudes (from 10^{-5} to 10^{-3}) on intrinsic term of martensite suggest that the loss factor decreases with the scanning speed and at strains higher than 10^{-4}. Near 10^{-5} the signal was quite unstable, however, it can be firstly assumed that the loss factor is independent from the *h* and *v* process parameters at such low strains. To entangle these behavior further investigations should be accounted.

5. Conclusions

A systematic investigation of damping properties of NiTi material produced via selective laser beam melting was presented. Damping was evaluated through the loss factor index considering both viscous (low strains) and energetic approaches (high strains). Results confirm that NiTi produced through SLM is an excellent candidate in substituting conventional materials when used in the martensite phase. At low strains, the loss factor index of martensite is maximized when h = 120 μm and v = 1500 mm/s. It varies in the [0.045 – 0.05] range and it is slightly dependent on the solicitation frequency. Furthermore, the transition into the rhombohedral phase allows the highest loss factor values, 0.0824, during cooling and with h = 120 μm and v = 1500 mm/s. At high strains, despite a stable and high recovered strain, the loss factor and the loss energy are low, suggesting that the as-built condition is not suitable for dynamic functioning at under this condition.

Supporting Information

Supporting Information is available from the Wiley Online Library or from the author.

Acknowledgements

Authors thank Mr. Bennato Nicola for his technical support in the fabrication of NiTi parts through SLM process.

Received: ((will be filled in by the editorial staff))

Revised: ((will be filled in by the editorial staff))

Published online: ((will be filled in by the editorial staff))

References

[1] K. Otsuka, X. Ren, *Progr. Mater. Sci.* **2005**, *50*, 511–678.

[2] S. C. Dutta, R. Majumder, *Shape Memory Alloy (SMA) as a Potential Damper in Structural Vibration Control*, *In: S. Hloch, D. Klichová, G. Krolczyk, S. Chattopadhyaya, L. Ruppenthalová (eds) Advances in Manufacturing Engineering and Materials. Lecture Notes in Mechanical Engineering*, Springer, Cham **2019**

[3] R. Lammering, I. Schmidt, *Smart Mater. Struct.* **2001**, *10*, 853–859.

[4] E. J. Graesser, *Metall. Mater. Trans. A* **1995**, *26A*, 2791.

[5] H. Soul, A. Isalgue, A. Yawny, V. Torra, F. C. Lovey, *Smart Mater. Struct.* **2010**, *19*, 085006.

[6] J. Van Humbeeck, S. Kustov, *Smart Mater. Struct.* **2005**, *14*, S171–S185.

[7] A. Nespoli, D. Rigamonti, M. Riva, E. Villa, F. Passaretti, *Smart Mater. Struct.* **2016**, *25*, 105001.

[8] Q.F. Chen, X.B. Zuo, L.M. Wang, W. Chang, W.Y. Tian, A.Q. Li, H. Yang, L.H. Liu, *Mater. Sci. Eng. A* **2006**, *438–440*, 1089–1092.

[9] J. San Juan, M.L. No´, *J. Alloys Compd.* **2003**, *355*, 65–71.

[10] J. Van Humbeeck, *J. Phys. IV* **1996**, *6*, 371-380.

[11] J. Van Humbeeck , *J. Alloys Compd.* **2003**, *355*, 58–64.

[12] X. Wang, M. Speirs, S. Kustov, B. Vrancken, X. Li, JP Kruth, J. Van Humbeeck, *Scripta Mater.* **2018**, *149*, 246-250.

[13] A. Nespoli, E. Bassani, D. Della Torre, R. Donnini, E. Villa, F. Passaretti, *Smart Mater. Struct.* **2017**, *26*, 105041.

[14] V. Torra, A. Isalgue, F. C. Lovey, M. Sade, *J. Therm. Anal. Calorim.* **2015**, *119*, 1475–1533.

[15] L. Dieng, G. Helbert, S. A. Chirani, T. Lecompte, P. Pilvin, *Eng. Struct.* **2013**, *56*, 1547–1556.

[16] V. C. de Sousa, C. De Marqui Junior, *J. Intell. Mater. Syst. Str.***2014**, *27(1)*, 117-133.

[17] E.T.F. Chau, C.M. Friend, D.M. Allen, J. Hora, J.R. Webster, *Mater. Sci. Eng. A* **2006**, *438–440*, 589–592.

[18] D. J. Hartl, D. C. Lagoudas, *J. Aerosp. Eng.* **2007**, *221*, 535-552.

[19] S. Barbarino, E. I. Saavedra Flores, R. M. Ajaj, I. Dayyani, M. I. Friswell, *Smart Mater. Struct.* **2014**, *23*, 063001.

[20] L. McDonald Schetky, *Mater. Des.* **1991**, *12*, 29-32.

[21] M. Carfagni, E. Lenzi, M. Pierini, *Proc. SPIE* **1998**, *3243*, 580-584.

[22] E. Kaya, I. Kaya, *Int. J. Adv. Manuf. Techn.* **2019**, *100*, 2045–2087.

[23] Y.Kaynak, H.Tobe, R.D. Noebe, H.E. Karaca, S. Jawahir, *Scripta Mater.* **2014**, *74*, 60-63.

[24] S.K Wu, H.C. Lin, C.C. Chen, *Mater. Letters* **1999**, *40*, 27-32.

[25] G. Wang, Z. Liu, W. Huang, B. Wang, J. Niu, *Int. J. Adv. Manuf. Technol.* **2019**, *102*, 2211–2221.

[26] K. Mehta, K. Gupta, *Machining of Shape Memory Alloys. In: Fabrication and Processing of Shape Memory Alloys.* Springer Briefs in Applied Sciences and Technology. Springer **2019**.

[27] A. Nespoli, D. Rigamonti, E. Villa, F. Passaretti, *Sens. Actuators A: Phys.* **2014**, *218*, 142-153.

[28] A. Nespoli, V. Dallolio, E. Villa, F. Passaretti, *Mater. Sci. Eng.: C* **2015**, *56*, 30-36.

[29] I. Yadroitsev, I. Smurov, *Phys. Procedia* **2010**, *5*, 551–560.

[30] E. Liverani, A. Fortunato, A. Leardini, C. Belvedere, S. Siegler, L. Ceschini, A. Ascari, *Mater. Des.* **2016**, *106*, 60-68.

[31] L. Mullen, R.C. Stamp, W. K. Brooks, E. Jones, C. J. Sutcliffe, *J. Biome. Mater. Res.* **2009**, *89(2)*, 325-334.

[32] M.H. Elahinia, M. Hashemi, M. Tabesh, S. B. Bhaduri, *Prog. Mater. Sci.* **2012**, *57*, 911-946.

[33] M. Seabra, J. Azevedo, A. Araújo, L. Reis, E. Pinto, N. Alves, R. Santos, J. P. Mortágua, *Proc. Struc. Integr.* **2016**, *1*, 289-296.

[34] I. Yadroitsev, P. Krakhmalev, I. Yadroitsava, *J. All. Comp.* **2014**, *583*, 404-409.

[35] J.M. Walker, C. Haberland, M.T. Andani, H. E. Karaca, D. Dean, M. Elahinia, *J. Intell. Mater. Struct.* **2016**, *27(19)*, 1-8.

[36] C. Haberland, M. Elahinia, J. M. Walker, H. Meier, J. Frenzel, *Smart Mater. Struct.* **2014**, *23*, 104002.

[37] S. Dadbakhsh, M. Speirs, J-P. Kruth, J. Schrooten, J. Luyten, J. Van Humbeeck, *Adv. Eng. Mater.* **2014**, *16(9)*, 1-7.

[38] N.S. Moghaddam, S. Saedi, A. Amerinatanzi, A. Hinojos, A. Ramazzani, J. Kudin, M.J. Mills, H. Karaca, M. Elahinia, *Scientific reports* **2019**, *9(41)*, 1-11.

[39] M. Speirs, X. Wang, S. Van Baelen, A. Ahadi, S. Dadbakhsh, J.P. Kruth, J. Van Humbeeck, *Shap. Mem. Superelasticity* **2016**, *2*, 310-316.

[40] X. Wang, J. Yu, J. Liu, L. Chen, Q. Yang, H. Wei, J. Sun, Z. Wang, Z. Zhang, G. Zhao, J. Van Humbeeck, *Addit. Manuf.* **2020**, *36*, 101545.

[41] E. Farber, J.N. Zhu, A. Popovich, V. Popovich, *Mater. Today: Proc.* **2020**, *30(3)*, 761-767.

[42] J.N. Zhu, E. Borisov, X. Liang, E. Farber, M.J.M. Hermans, V.A. Popovich, *Addit. Manuf.* **2021**, *38*, 101802.

[43] X. Wang, S. Kustov, J. Van Humbeeck, *Mater.* **2018**, *11*, 1683.

[44] S. Saedi, A.S. Turabi, M.T. Andani, C. Haberland, M. Elahinia, H. Karaca, *Smart Mater. Struct*. **2016**, *25*, 035005.

[45] M.T. Andani, S. Saedi, A.S. Turabi, M.R. Karamooz, C. Haberland, H.E. Karaca, M. Elahinia, *J. Mech. Behavior Biom. Mater.* **2017**, *68*, 224-231.

[46] S. Saedi, N.S. Moghaddam, A. Amerinatanzi, M. Elahinia, H.E. Karaca, *Acta Mater*. **2018**, *144*, 552-560.

[47] H. Meier, C. Haberland, J. Frenzel, *Structural and Functional Properties of NiTi Shape Memory Alloys Produced by Selective Laser Melting. In: Innovative Developments in Design and Manufacturing: Advanced Research in Virtual and Rapid Prototyping*. Paulo Jorge Bartolo et al., Taylor and Francis Group, London pp 291-296, **2011**.

[48] A. Nespoli, A.M. Grande, N. Bennato, D. Rigamonti, P. Bettini, E. Villa, G. Sala, F. Passaretti, *Prog. Addit. Manuf*. **2020**, 1-17.

[49] R. C. Crăciun, S. Stanciu, R. Cimpoeșu, A. I. Ursanu, V. Manole, P. Paraschiv, D. L. Chicet, *Mater. Sci. Eng.* **2016**, *147*, 012031.

[50] F. Aggogeri, A. Borboni, A. Merlo, N. Pellegrini, R. Ricatto, Mater. 2017, 10, 297.

[51] Y. Yan, H. Yin, Q. P. Sun, Y. Huo, *Continuum Mech. Thermodyn.* **2012**, *24*, 675.

[52] H. Yin, Y. He, Q. Sun, J. Mech. Phys. Solids, 2014, 67, 100-128.

This is the accepted version of:
A. Nespoli, P. Bettini, E. Villa, G. Sala, F. Passaretti, A.M. Grande
A Study on Damping Property of Niti Elements Produced by Selective Laser-Beam Melting
Advanced Engineering Materials
doi:10.1002/adem.202001246
The final publication is available at https://doi.org/10.1002/adem.202001246

Figure 1. Internal friction IF(T) measurement at low strain with indication of the different contributions (a) and pseudoelastic stress-strain curve (b).

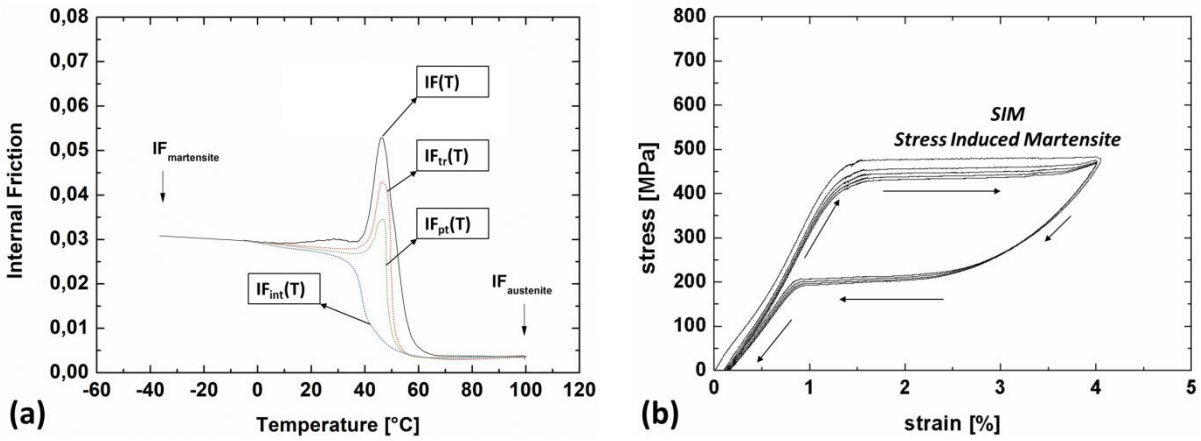

Figure 2. Intrinsic internal friction of martensite: loss factor maps as a function of the SLM process parameters (hatching and scanning speed) of martensite at 0.5 Hz (a), 1 Hz (b) and 10 Hz (c), at 0.02% cyclic strain (T = -70 °C).

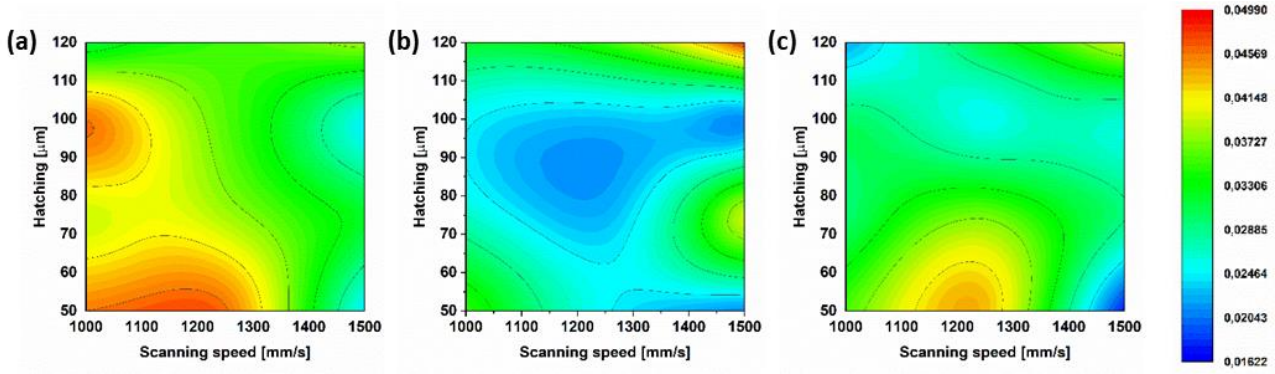

This is the accepted version of:
A. Nespoli, P. Bettini, E. Villa, G. Sala, F. Passaretti, A.M. Grande
A Study on Damping Property of Niti Elements Produced by Selective Laser-Beam Melting
Advanced Engineering Materials
doi:10.1002/adem.202001246
The final publication is available at https://doi.org/10.1002/adem.202001246

Figure 3. Intrinsic internal friction of austenite: loss factor maps as a function of the SLM process parameters (hatching and scanning speed) of austenite at 0.5 Hz (a), 1 Hz (b) and 10 Hz (c), at 0.02% cyclic strain (T = 130 °C).

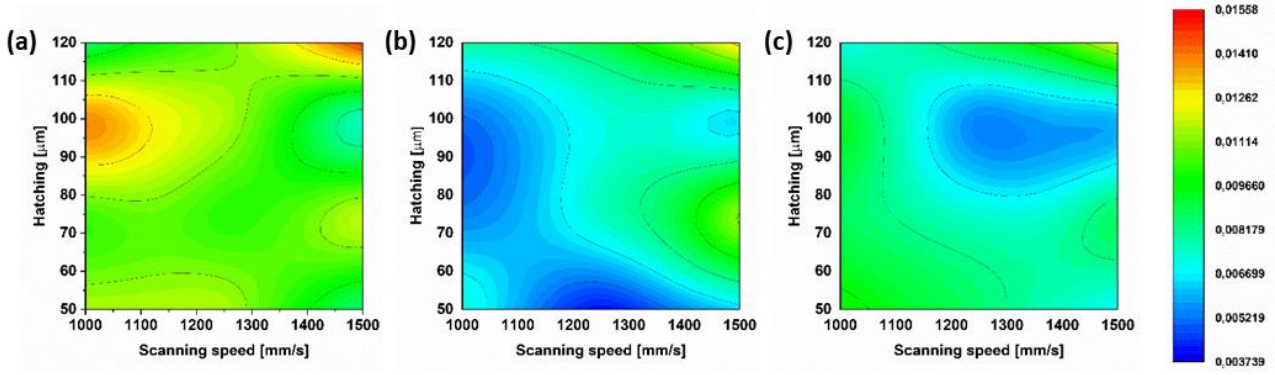

Figure 4. Martensite loss factor *vs*. solicitation strain at 10 Hz of samples fabricated with *h* = 50 µm (a), 75 µm (b), 100 µm (c), 120 µm (d).

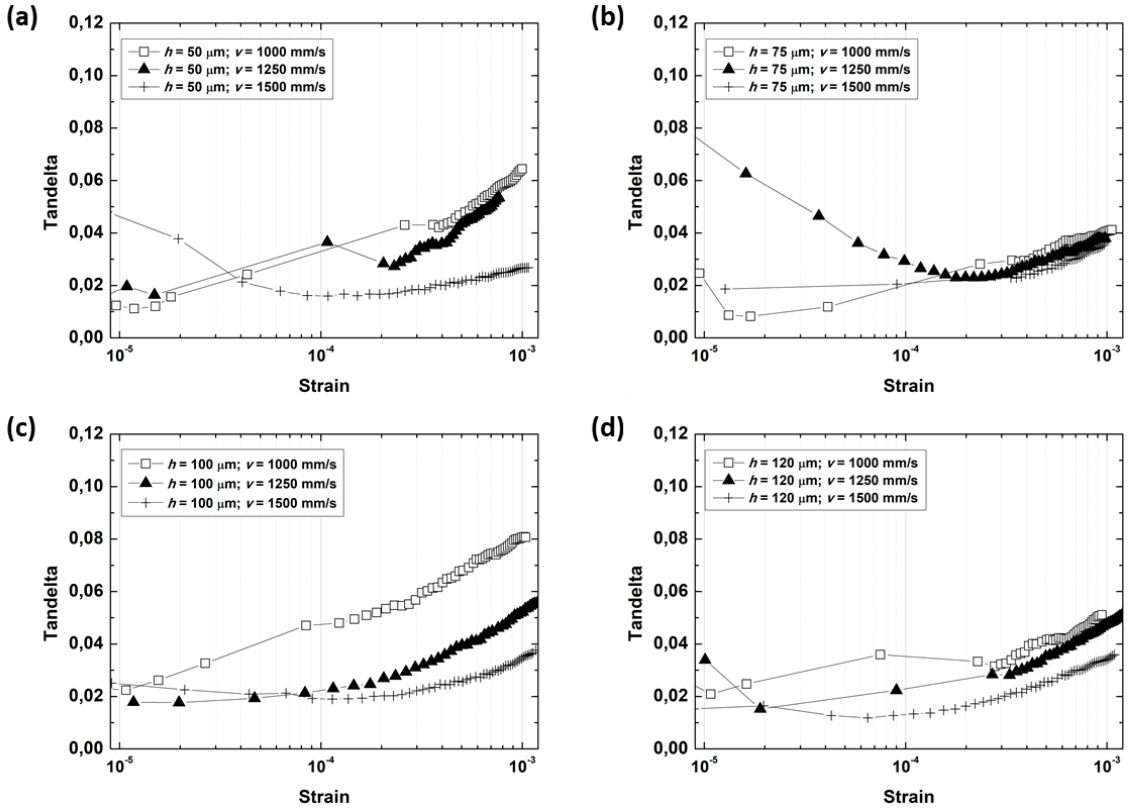

This is the accepted version of:
A. Nespoli, P. Bettini, E. Villa, G. Sala, F. Passaretti, A.M. Grande
A Study on Damping Property of Niti Elements Produced by Selective Laser-Beam Melting
Advanced Engineering Materials
doi:10.1002/adem.202001246
The final publication is available at https://doi.org/10.1002/adem.202001246

Figure 5. Compression test at 1 Hz on sample fabricated with hatching distance = 100 µm and scanning speed = 1000 mm/s.

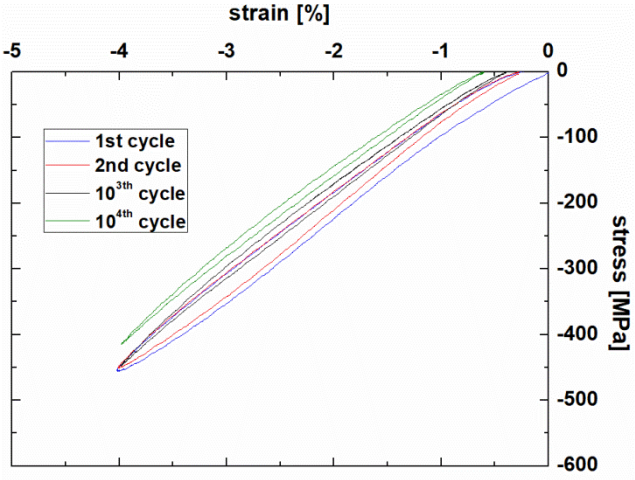

Figure 6. Loss factor maps as a function of the SLM process parameters (hatching and scanning speed) at 50 (a), 1000 (b) and 10000 (c) loading cycles during the compression tests at 1 Hz and A_f + 10 °C.

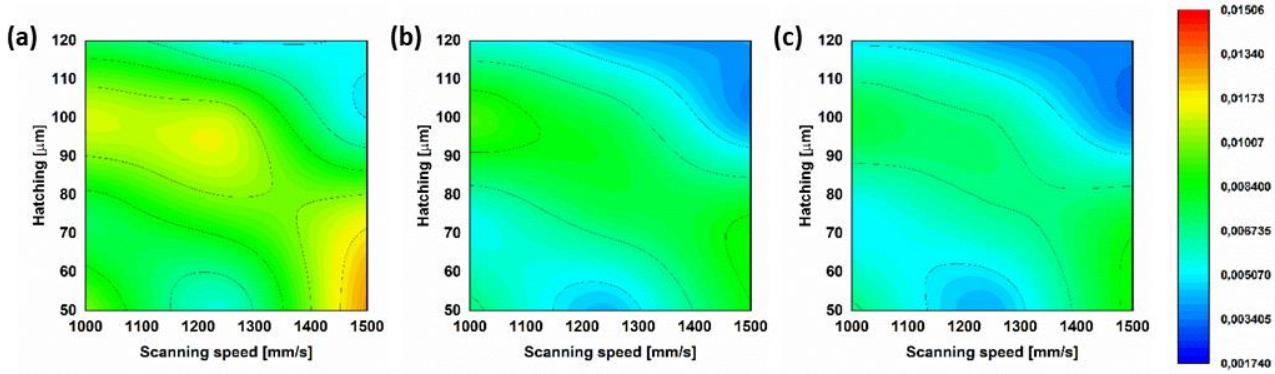

This is the accepted version of:
A. Nespoli, P. Bettini, E. Villa, G. Sala, F. Passaretti, A.M. Grande
A Study on Damping Property of Niti Elements Produced by Selective Laser-Beam Melting
Advanced Engineering Materials
doi:10.1002/adem.202001246
The final publication is available at https://doi.org/10.1002/adem.202001246

Figure 7. Loss factor maps as a function of the SLM process parameters (hatching and scanning speed) at 50 (a), 1000 (b) and 10000 (c) loading cycles during the compression tests at 3.5 Hz and A_f + 10 °C.

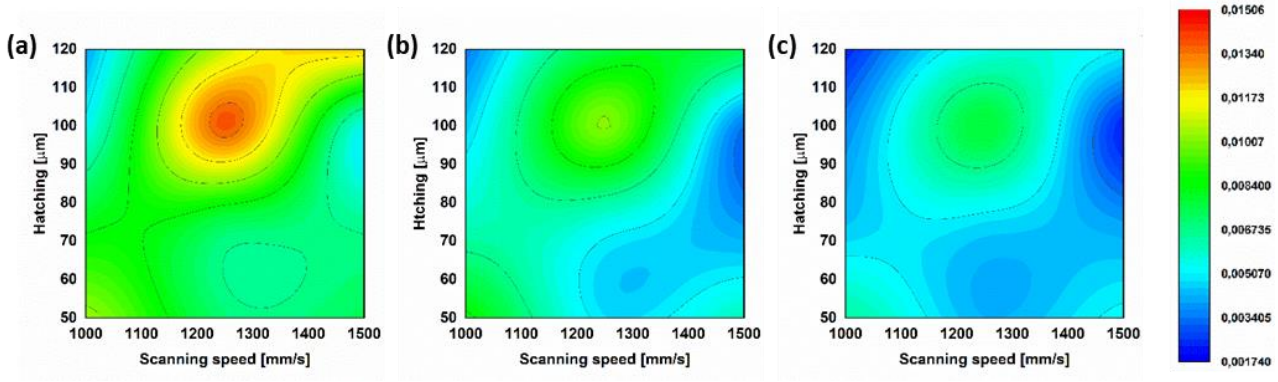

Figure 8. Comparison between maximum loss factor of NiTi fabricated through selective laser beam melting (SLM) and other materials obtained from conventional processing. Green bars represent the results of the present study.

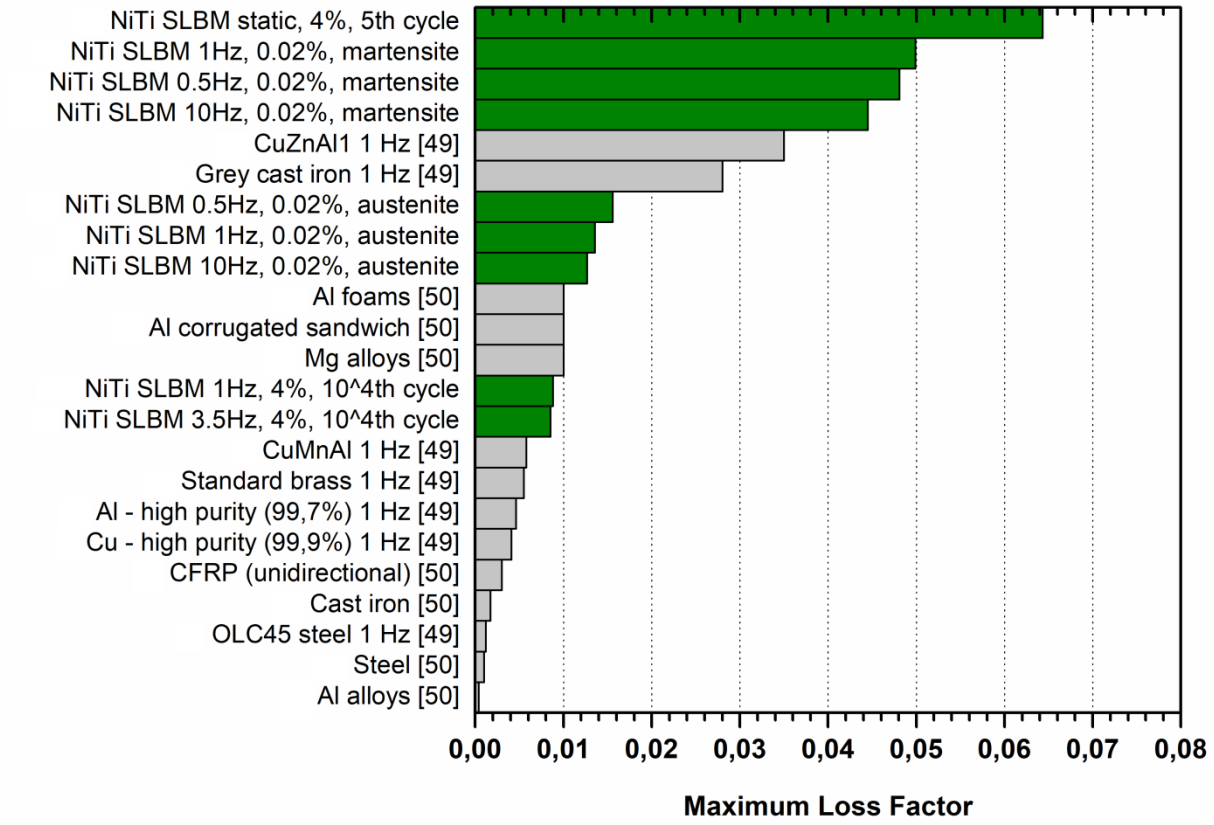

Figure 9. Comparison between quasi-static (a) and 1 Hz (b) responses of sample fabricated with hatching distance = 100 µm and scanning speed = 1000 mm/s (the first five mechanical cycles are reported).

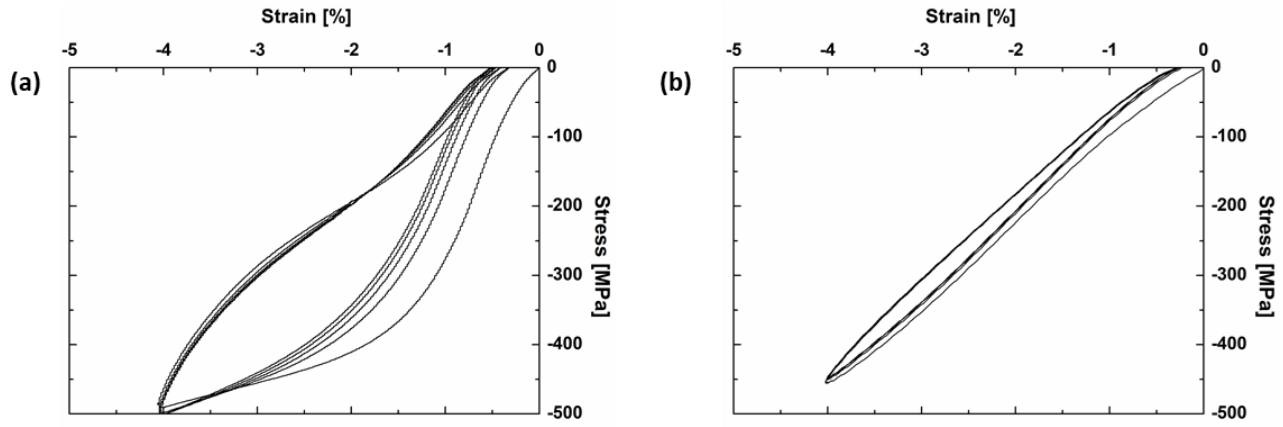

This is the accepted version of:
A. Nespoli, P. Bettini, E. Villa, G. Sala, F. Passaretti, A.M. Grande
A Study on Damping Property of Niti Elements Produced by Selective Laser-Beam Melting
Advanced Engineering Materials
doi:10.1002/adem.202001246
The final publication is available at https://doi.org/10.1002/adem.202001246

Table 1. SLM process parameters and Af temperature of the twelve families.

NiTi family	Hatching [µm]	Scanning speed [mm/s]	Af [°C]
1	50	1000	51
2	50	1250	80
3	50	1500	72
4	75	1000	63
5	75	1250	66
6	75	1500	57
7	100	1000	45
8	100	1250	65
9	100	1500	90
10	120	1000	55
11	120	1250	62
12	120	1500	65

Table 2. *h* and *v* process parameters that maximize the loss factor.

		h **[µm]; *v* [mm/s]**
Low strain (10^{-4})	**NiTi SLBM - 0.5hz martensite**	100; 1000
	NiTi SLBM - 0.5hz austenite	120; 1500
	NiTi SLBM - 1hz martensite	120; 1500
	NiTi SLBM - 1hz austenite	120; 1500
	NiTi SLBM - 10hz martensite	50; 1250 and 120; 1500
	NiTi SLBM - 10hz austenite	120; 1500
	NiTi SLBM – phase transition term - cooling	120; 1250
	NiTi SLBM – phase transition term - heating	50; 1000 and 120; 1500
High strain	**NiTi SLBM - 1hz, 4% strain, 10^4th cycle**	100; 1000
	NiTi SLBM - 4hz, 4% strain, 10^4th cycle	50; 1500 and 100; 1250
	NiTi SLBM - static, 4% strain, 5th cycle	120; 1250

This is the accepted version of:
A. Nespoli, P. Bettini, E. Villa, G. Sala, F. Passaretti, A.M. Grande
A Study on Damping Property of Niti Elements Produced by Selective Laser-Beam Melting
Advanced Engineering Materials
doi:10.1002/adem.202001246
The final publication is available at https://doi.org/10.1002/adem.202001246

Table of contents

The paper presents an overview of the dynamic damping properties of NiTi samples fabricated through selective laser beam melting. Results show that the printed parts have a peculiar damping response depending on the selected process parameters and higher than that registered for conventional metals.

Adelaide Nespoli, Paolo Bettini, Elena Villa, Giuseppe Sala, Francesca Passaretti, Antonio Mattia Grande*

A study on damping property of NiTi elements produced by selective laser beam melting

Title

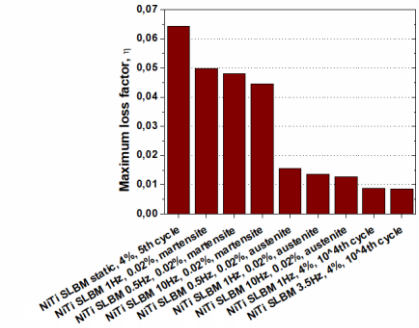

This is the accepted version of:
A. Nespoli, P. Bettini, E. Villa, G. Sala, F. Passaretti, A.M. Grande
A Study on Damping Property of Niti Elements Produced by Selective Laser-Beam Melting
Advanced Engineering Materials
doi:10.1002/adem.202001246
The final publication is available at https://doi.org/10.1002/adem.202001246

Supporting Information

A study on damping property of NiTi elements produced by selective laser beam melting

Adelaide Nespoli, Paolo Bettini, Elena Villa, Giuseppe Sala, Francesca Passaretti, Antonio Mattia Grande*

Figure S1. Loss energy [J] maps as a function of the SLM process parameters (hatching and scanning speed) at 50 (a), 1000 (b) and 10000 (c) loading cycles during the compression tests at 1 Hz and A_f + 10 °C.

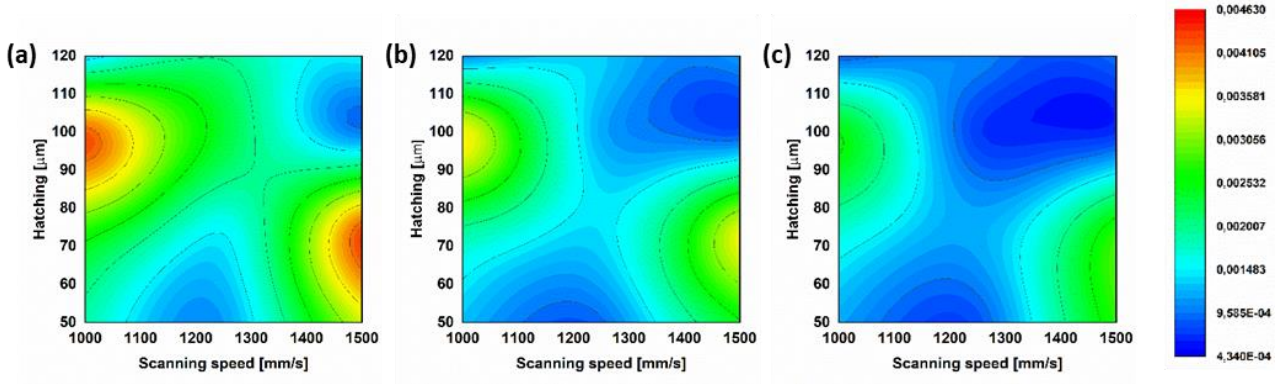

Figure S2. Loss energy maps [J] as a function of the SLBM process parameters (hatching and scanning speed) at 50 (a), 1000 (b) and 10000 (c) loading cycles during the compression tests at 3.5 Hz and A_f + 10 °C.